Hindawi Publishing Corporation
EURASIP Journal on Wireless Communications and Networking
Volume 2010, Article ID 232754, 10 pages
doi:10.1155/2010/232754

Research Article

Advances in Relay Networks: Performance and Capacity Analysis of Space-Time Analog Network Coding

Shujaat Ali Khan Tanoli,[1] Imran Khan,[1] Nandana Rajatheva,[1] and Fumiyuki Adachi[2]

[1] *School of Engineering and Technology, Asian Institute of Technology Pathumthani 12120, Thailand*
[2] *Graduate School of Engineering, Tohoku University, Sendai 9808579, Japan*

Correspondence should be addressed to Shujaat Ali Khan Tanoli, shujaat.ali.khan@ait.ac.th and Imran Khan, imrankhan@nwfpuet.edu.pk

Received 20 July 2010; Revised 31 October 2010; Accepted 10 December 2010

Academic Editor: Stefan Kaiser

We propose modified space-time-coding-based analog network coding (ANC) for multiple-relay network, termed space-time analog network coding (STANC). We present the performance and capacity analysis of the proposed network in terms of SER and ergodic capacity. We derive the closed-form expressions for the moment-generating function (MGF) of the equivalent signal-to-noise ratio (SNR) of the multiple-relay STANC network over independent and identically distributed (i.i.d.) Rayleigh, Nakagami, and Rician channels. Average SER of the system is evaluated using MGF-based approach. We further derive the approximate closed-form expressions of ergodic capacity. These expressions are simple and enable effective evaluation of the performance and capacity of STANC system.

1. Introduction

Relay nodes are considered as the main candidates for long-term-evolution-(LTE-) advanced standardization to provide incremental capacity growth and in-building coverage [1]. IEEE 802.16j standardization is developed for cooperative techniques to describe different modes of operation and frame structures [2]. In addition to the various advancements in the field of relay networks, it has also become vital to apply channel coding techniques to achieve high capacity and coding gain. Methods for implementing code diversity in fading scenario using higher-order coded modulation schemes are reported in [3, 4]. The idea of network coding (NC) was first introduced by Ahlswede et al. [5] to enhance the capacity of the wired networks. The essential idea of NC was further extended to wireless networks to explore the broadcast nature of wireless medium and to yield significant performance improvements in the wireless networks [5]. In [6–9], authors analyze the bit error rate (BER) and network capacity of physical-layer network coding (PNC) for frequency flat-fading channel and report that the capacity of bidirectional communication in a cooperative transmission (CT) increases by employing PNC. In PNC, the logical operation, that is XOR, is used by relay to map received signal into a digital bit stream, so that the interference becomes part of the arithmetic operation in network coding. In analog network coding (ANC), the relay simply amplifies and broadcasts the received signal without any processing.

The interference is always considered as a most harmful factor for wireless transmission. Wireless networks attempt to avoid scheduling multiple transmissions at the same time in order to prevent interference. Analog network coding (ANC), recognized as a variant of PNC, follows the opposite approach, which strategically allows the selected senders to interfere in order to exploits interference instead of avoiding it. The concept of ANC was first proposed by the author of [10], in which the terminals are allowed to simultaneously transmit their signals. The wireless channel naturally combines the signals, and the relay amplifies and forwards the resultant signal instead of forwarding combined packets as in digital network coding. The potential of analog network coding is recognized in information theory where it almost doubles the canonical relay network capacity in comparison with the conventional point-to-point transmission

[10–12]. However, most of the research works reported in the literature so far focus only on the capacity bounds and do not provide the theoretical performance bound for symbol error rate (SER). In [7], an algorithm for PNC was proposed with certain assumptions of synchronization; symbol level, phase, and frequency. To make it more practical, the authors of [10] introduced an algorithm without those assumptions to exploit the lack of synchronization between interfering signals. In [13], the authors investigated the broadband bidirectional transmission with ANC scheme based on OFDM radio access in a frequency-selective fading channel. Most recently, a differential modulation scheme is proposed for analog network coding (ANC-DM) in which the channel state information (CSI) is not required at both sources and the relay [14], but the differential scheme is about 3 dB away as compared with the coherent detection scheme.

This paper presents the novel extension of analog network coding based on space-time coding technique (STANC) in a multihop scenario in view of further enhancing the network capacity and coverage area. In STANC, two terminals transmit their signals at the same instant to L number of relays, and each relay forwards the amplified version of the signal (the sum of signals from both terminals as received at the relay) to both the terminals in the second phase. Both terminals transmit signals simultaneously as discussed in [15]. Each signal takes two time slots to reach the destination terminal with the same throughput as in ANC but with improved performance. Although our work builds on earlier work, it exploits the space diversity by involving space time coding as a new aspect. We derive the theoretical closed-form expressions of moment-generating function (MGF) for STANC system over Nakagami-m and Rician fading channels. Further, we analyze the performance of STANC in terms of SER using the MGF-based approach. The approximate closed-form expressions of ergodic capacity over both Nakagami-m and Rician fading channels are derived.

This paper is organized as follows: Section 2 introduces the system model, channel model, transmission protocol, and equivalent SNR. Section 3 gives detailed derivations of closed-form MGF expressions. Section 4 presents the approximate closed-form expressions of ergodic capacity for both Nakagami and Rician distributions. Section 5 discusses the analytical and simulation results of the system performance. Finally, Section 6 concludes the paper.

Notations. $\mathbb{E}(\cdot)$, $|\cdot|$, $\Gamma(\cdot)$, and $\psi(\cdot,\cdot,\cdot)$ denote the expectation operator, the magnitude of complex value, the gamma function, and confluent hypergeometric function of the second kind, respectively. $X \rightarrow Y$ describes the link from node X to Y. α_{ij}, K_{ij}, and m represent the multipath gain coefficient, Rician-K factor, and the Nakagami-m factor, respectively from ith terminal to jth relay. E_x, γ_i, $\mathcal{M}_{\gamma_i}(s)$, and n_{xk} represent the transmitted symbol energy of terminal X over $X \rightarrow Y$ link, equivalent signal-to-noise ratio (SNR) at ith terminal, total unconditional moment-generating function of γ_i, and AWGN at terminal X in the qth time slot, respectively. T_i and R_j denote the ith terminal and jth relay, respectively.

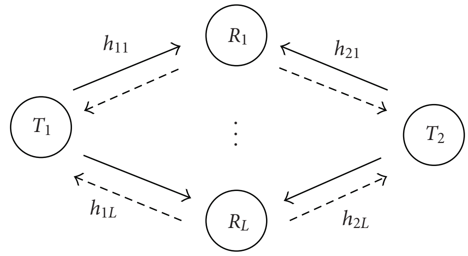

Figure 1: STANC system model.

2. System Model

The STANC cooperation model is shown in Figure 1. The terminals T_1 and T_2 communicate with each other through an L number of relays R_j, where $j = 1, 2, \ldots, L$. All the terminals are equipped with a single antenna and the relays operate in amplify-and-forward mode.

2.1. Channel Model. It is assumed that the channel fading coefficients will remain the same for the two phases. It is also assumed that the transmitter (source terminal) has no channel information, but only the receiver (destination terminal) has perfect channel state information (CSI), which can be acquired by applying the training-based channel estimation schemes as reported in [16], where the entire channel link from source terminal to destination terminal is only estimated at the destination terminal. Here, we assume identical and independently distributed (i.i.d) Nakagami-m fading channels and Rician fading channels for all the links between terminals and relay. h_{ij} is the fading magnitude of the link between ith terminal and jth relay. $\alpha_{ij} = |h_{ij}|^2$ ($i = \{1, 2\}$ and $j = \{1, 2, \ldots, L\}$) are gamma-distributed random variables. The probability density function of α_{ij} for Nakagami-m distribution is given in [17] as

$$f\left(\alpha_{ij}\right) = \frac{m^m \alpha_{ij}^{m-1}}{\Gamma(m)} \exp\left(-m\alpha_{ij}\right), \quad (1)$$

where $\Gamma(\cdot)$ is a gamma function. Here, we consider $\mathbb{E}(|h_{ij}|^2) = 1$, where $\mathbb{E}(\cdot)$ is the expectation operator. For $m = 1$ the Nakagami-m distribution becomes the exponential distribution.

Using [18, equation (2.15)], the probability density function of α_{ij} for Rician distribution is given as:

$$f\left(\alpha_{ij}\right) = \left(1 + K_{ij}\right) \exp\left(-\left(1 + K_{ij}\right)\alpha_{ij} - K_{ij}\right) \times I_0\left(2\sqrt{\left(K_{ij}\left(1 + K_{ij}\right)\right)\alpha_{ij}}\right), \quad (2)$$

where $I_0(\cdot)$ is the zero-th order modified Bessel function of the first kind and K_{ij} is the Rician fading factor for the link from ith to jth terminal. For $K_{ij} = 0$, the Rician distribution becomes the Rayleigh distribution.

Table 1: STANC transmission protocol.

Time Slot 1	Time Slot 2
$T_1, T_2 \rightarrow R_j$	$R_j \rightarrow T_1, T_2$

2.2. STANC Transmission Protocol. The signaling in the proposed protocol is explained in Table 1. x_{ik} represents the signal of kth symbol from ith terminal. For the basic analog network coding scheme (ANC) [13] as given in Table 1, the R_j denotes jth relay, (where $j = \{1, 2, \ldots, L\}$) and L is the total number of relays. $L = 1$ implies that the system uses the basic ANC scheme without STC. As the number of relays increases, the system starts using STANC based on STC codes and orthogonal STANC (OSTANC) based on OSTBC codes. Further, we compare the basic ANC scheme with STANC and OSTANC in terms of the three cases listed below.

(i) Case A: 2-relay STANC.

(ii) Case B: 3-relay OSTANC.

(iii) Case C: L-relay STANC (general condition).

Case A. The Alamouti code for ith terminal is given as

$$\mathbf{C_i} = \begin{pmatrix} x_{i1} & x_{i2} \\ -x_{i2}^* & x_{i1}^* \end{pmatrix}. \quad (3)$$

Terminals T_1 and T_2 send x_{11} and x_{21}, respectively, to R_1 in first time slot and x_{12} and x_{22}, respectively, to R_2 in second time slot. The ANC scheme exploits the interference of the simultaneously transmitted signals in wireless channels. Therefore, in third time slot, R_1 and R_2 amplify and forward the received signals to both T_1 and T_2 on two orthogonal channels (FDMA-based rather than TDMA). In the fourth time slot, T_1 and T_2 send $-x_{12}^*$ and $-x_{22}^*$, respectively, to R_1, and x_{11}^* and x_{21}^*, respectively, to R_2 in fifth time slot. In sixth time slot, R_1 and R_2 amplify the information and the combined signals are forwarded to T_1 and T_2 through orthogonal subcarriers.

Case B. For simplicity, we assume 4×3 OSTBC for ith terminal by considering three-relay ANC scenario.

$$\mathbf{C_i} = \begin{pmatrix} x_{i1} & x_{i2} & x_{i3} \\ -x_{i2}^* & x_{i1}^* & 0 \\ x_{i3}^* & 0 & -x_{i1}^* \\ 0 & x_{i3}^* & -x_{i2}^* \end{pmatrix}_{4\times 3}. \quad (4)$$

We focus only on the message sent by the source terminal T_1 to the destination terminal T_2 through R_1, R_2, and R_3. In first, second, and third time slots, terminal T_1 transmits signal x_{11}, x_{12}, and x_{13} to R_1, R_2, and R_3, respectively. In fourth time slot, the relays retransmit the combined signals to both the terminals through orthogonal channels.

In fifth and sixth time slots, T_1 transmits $-x_{12}^*$ to R_1 and x_{11}^* to R_2, respectively. In seventh time slot, R_1 and R_2 forward the scaled received signals to T_2. Similarly, in eighth, ninth, and tenth time slots, x_{13}^* and $-x_{11}^*$ are transmitted to T_2 through R_1 and R_3, respectively. In eleventh, twelfth, and thirteenth time slots, signals x_{13}^* and $-x_{12}^*$ are transmitted through R_2 and R_3, respectively, to terminal T_2.

Case C. In orthogonal transmission, the number of time slots increases with the increase in the number of transmitted symbols. The general form of OSTBC is given in [19] as:

$$\mathbf{C} = \begin{pmatrix} x_{11}(1) & x_{12}(1) & \ldots & x_{1L}(1) \\ x_{11}(2) & x_{12}(2) & \ldots & x_{1L}(2) \\ \vdots & \vdots & \ddots & \vdots \\ x_{11}(t) & x_{12}(t) & \ldots & x_{1L}(t) \end{pmatrix}_{t\times L}, \quad (5)$$

where t is the total number of time slots used by L number of relays.

2.3. Input-Output Equations

Case A. The signals x_{i1} and x_{i2} are transmitted by T_i (where $i \in \{1, 2\}$) to the relays R_1 and R_2, respectively. The signals received at R_1 and R_2 are given by:

$$\begin{aligned} y_{r_1} &= h_{11}\sqrt{E_1}x_{11} + h_{21}\sqrt{E_2}x_{21} + n_{r_1}, \\ y_{r_2} &= h_{12}\sqrt{E_1}x_{12} + h_{22}\sqrt{E_2}x_{22} + n_{r_2}, \end{aligned} \quad (6)$$

where $n_{r_j} \sim \mathcal{CN}(0, N_0)$ and E_i is the transmitted symbol energy at ith terminal.

The jth relay normalizes the received signal by a factor of $\sqrt{E(|y_{r_j}|^2)}$ and transmits the analog network coded signal to $T_1$and T_2. The amplification factor (β_j) at the jth relay is given by

$$\beta_j = \sqrt{\frac{E_{r_j}}{E_1 + E_2 + N_0}}, \quad (7)$$

where E_{r_j} is the average transmitted symbol energy at R_j. The two terminals T_i $(i \in \{1, 2\})$ receive the signal from jth relay through two orthogonal channels and the general form of received signal is given as:

$$r_{ij} = h_{ij}\beta_j y_{r_j} + n_i, \quad (8)$$

where $n_i \sim \mathcal{CN}(0, N_0)$ at ith terminal T_i. T_i knows x_{i1} and h_{ij}. We assume that each terminal knows the value of β_j. Knowing all these values, the terminals T_1 and T_2 can recover the data by removing their self information as given below:

$$y_{ij} = r_{ij} - \left|h_{ij}\right|^2 \beta_j \sqrt{E_i} x_{ik}. \quad (9)$$

Hence, the recovered signals from both the relays can be written as:

$$\begin{aligned} y_{11} &= \beta_1 h_{11} h_{21}\sqrt{E_2}x_{21} + \tilde{n}_{11}, \\ y_{12} &= \beta_2 h_{12} h_{22}\sqrt{E_2}x_{22} + \tilde{n}_{12}, \\ y_{21} &= \beta_1 h_{11} h_{21}\sqrt{E_1}x_{11} + \tilde{n}_{21}, \\ y_{22} &= \beta_2 h_{12} h_{22}\sqrt{E_1}x_{12} + \tilde{n}_{22}, \end{aligned} \quad (10)$$

where $\tilde{n}_{ij} = \beta_j h_{ij} n_{r_j} + n_i$, having variance $(\beta_j^2 |h_{ij}|^2 + 1)N_0$.

Similarly, the signals $-x_{i2}^*$ and x_{i1}^* are transmitted by T_i (where $i \in \{1,2\}$) to the relays R_1 and R_2, respectively. The signals received at ith terminal through R_1 and R_2 are given by:

$$\begin{aligned} y_{11}^* &= -\beta_1 h_{11} h_{21}\sqrt{E_2}x_{22}^* + \tilde{n}_{11}^*, \\ y_{12}^* &= \beta_2 h_{12} h_{22}\sqrt{E_2}x_{21}^* + \tilde{n}_{12}^*, \\ y_{21}^* &= \beta_1 h_{11} h_{21}\sqrt{E_1}x_{12}^* + \tilde{n}_{21}^*, \\ y_{22}^* &= -\beta_2 h_{12} h_{22}\sqrt{E_1}x_{11}^* + \tilde{n}_{22}^*, \end{aligned} \tag{11}$$

where $\tilde{n}_{ij}^* = \beta_j h_{ij} n_{ij} + n_i$, having variance $(\beta_j^2|h_{ij}|^2 + 1)N_0$. The received signals at T_2 can be written in matrix form as:

$$\mathbf{Y} = \mathbf{H}\mathbf{X} + \acute{\mathbf{N}}, \tag{12}$$

where

$$\begin{aligned} \mathbf{Y}^T &= \begin{pmatrix} y_{21} & y_{22} & y_{21}^* & y_{22}^* \end{pmatrix}_{1\times 4}, \\ \mathbf{H}^T &= \begin{pmatrix} A_{21} & 0 & A_{22}^* & 0 \\ 0 & A_{22} & 0 & -A_{21}^* \end{pmatrix}_{2\times 4}, \\ \mathbf{X}^T &= \begin{pmatrix} x_{11} & x_{12} \end{pmatrix}_{1\times 2}, \\ \acute{\mathbf{N}}^T &= \begin{pmatrix} n_{21} & n_{22} & n_{22}^* & n_{21}^* \end{pmatrix}_{1\times 4} \end{aligned} \tag{13}$$

and $A_{21} = (\beta_1/\omega_{21})h_{11}h_{21}\sqrt{E_1}$, $A_{22} = (\beta_2/\omega_{22})h_{12}h_{22}\sqrt{E_1}$, where $\omega_{ij} = \sqrt{(\beta_j^2|h_{ij}|^2 + 1)}$ is a normalizing factor at the receiver. By multiplying $\mathbf{H}^H$ on both side of (12), we arrive at:

$$\mathbf{H}^H\mathbf{Y} = \left(|A_{21}|^2 + |A_{22}|^2\right)\begin{pmatrix} x_{11} \\ x_{12} \end{pmatrix} + \mathbf{H}^H\acute{\mathbf{N}}. \tag{14}$$

Case B. Using the TDMA-based protocol for the OSTANC system, the received signal from T_i at R_j in qth time slot is given as

$$y_{r_j} = \sum_{i=1}^{2} h_{ij}\sqrt{E_i}x_{ij} + n_{r_j}, \tag{15}$$

where $n_j \sim CN(0, N_0)$. The relays R_j normalize the received signal by a factor $\sqrt{E(|y_{ij}|^2)}$ and transmit the analog network coded signal to both the terminals T_i. The two terminals T_i ($i \in \{1,2\}$) receive the signals from the relays through three orthogonal channels, and the general form of received signal is given as:

$$r_{ij} = h_{ij}\beta_j y_{r_j} + n_i, \tag{16}$$

where $n_{ij} \sim \mathcal{CN}(0, N_0)$ at ith terminal T_i. T_i knows x_{ij} and h_{ij}. We assume that each terminal knows the value of β_j. Knowing all these values, the terminal T_1 amd T_2 can recover the data x_{2j} and x_{1j}, respectively, and the received signals can be written in matrix form as

$$\mathbf{Y} = \mathbf{H}\mathbf{X} + \acute{\mathbf{N}}, \tag{17}$$

where $\mathbf{Y}$, $\mathbf{H}$, $\mathbf{X}$, and $\acute{\mathbf{N}}$ are given as

$$\begin{aligned} \mathbf{Y}^T &= \begin{pmatrix} y_{21} & y_{22} & y_{23} & y_{22_1}^* & y_{21_1}^* & y_{23_1}^* & y_{21_2}^* & y_{23_2}^* & y_{22_2}^* \end{pmatrix}_{1\times 9} \\ \mathbf{H}^T &= \begin{pmatrix} A_{21} & 0 & 0 & A_{22}^* & 0 & -A_{23}^* & 0 & 0 & 0 \\ 0 & A_{22} & 0 & 0 & -A_{21}^* & 0 & 0 & -A_{23}^* & 0 \\ 0 & 0 & A_{23} & 0 & 0 & 0 & A_{21}^* & 0 & A_{22}^* \end{pmatrix}_{3\times 9} \\ \mathbf{X}^T &= \begin{pmatrix} x_{11} & x_{12} & x_{13} \end{pmatrix}_{1\times 3} \\ \acute{\mathbf{N}}^T &= \begin{pmatrix} n_{21} & n_{22} & n_{23} & n_{22_1}^* & n_{21_1}^* & n_{23_1}^* & n_{21_2}^* & n_{23_2}^* & n_{22_2}^* \end{pmatrix}_{1\times 9} \end{aligned} \tag{18}$$

$A_{1j} = (\beta_j/\omega_{1j})h_{1j}h_{2j}\sqrt{E_2}$, and $A_{2j} = (\beta_j/\omega_{2j})h_{1j}h_{2j}\sqrt{E_1}$, where $\omega_{ij} = \sqrt{(\beta_j^2|h_{ij}|^2 + 1)}$ is a normalizing factor at the receiver. The equivalent SISO model is obtained by premultiplying with $\mathbf{H}^H$ both sides of (18).

$$\begin{pmatrix} y_{21} \\ y_{22} \\ y_{23} \end{pmatrix} = \left(\sum_{j=1}^{3}\left|A_{2j}\right|^2\right)\begin{pmatrix} x_{11} \\ x_{12} \\ x_{13} \end{pmatrix} + \mathbf{H}^H\acute{\mathbf{N}}. \tag{19}$$

Case C. Similarly, the equivalent SISO model obtained for L number of relays is given as:

$$\begin{pmatrix} y_{21} \\ y_{22} \\ \vdots \\ y_{2L} \end{pmatrix} = \left(\sum_{j=1}^{L}\left|A_{2j}\right|^2\right)\begin{pmatrix} x_{11} \\ x_{12} \\ \vdots \\ x_{1L} \end{pmatrix} + \mathbf{H}^H\acute{\mathbf{N}}. \tag{20}$$

3. Performance Analysis

3.1. STANC Equivalent SNR. At terminal T_i, maximal ratio combining (MRC) is used to combine the signals received from L relays. In general, the STANC equivalent SNR at ith terminal can be expressed as:

$$\gamma_i = \frac{1}{N_0}\sum_{j=1}^{L}\left|A_{ij}\right|^2 = \sum_{j=1}^{L}\frac{\overline{\gamma}\beta_j^2\left|h_{1j}\right|^2\left|h_{2j}\right|^2}{\beta_j^2\left|h_{ij}\right|^2 + 1}, \tag{21}$$

where $\overline{\gamma} = E/N_0$ and $E = E_1 = E_2$. Here, $L = 2$ and $L = 3$ give the equivalent SNR for Cases A and B, respectively.

3.2. Average SER. The SER equations (P_e) for M-PSK and M-QAM modulation are as given below.

(1) M-PSK: the average SER for M-PSK is given in [18] as:

$$P_{e(\text{MPSK})} = \frac{1}{\pi}\int_0^{(M-1)\pi/M}\mathcal{M}_{\gamma_i}\left(\frac{g_{\text{PSK}}}{\sin^2\theta}\right)d\theta, \tag{22}$$

where $g_{\text{PSK}} = \sin^2(\pi/M)$.

(2) M-QAM: the average SER for M-QAM is given in [18] as:

$$P_{e(\text{MQAM})} = \frac{4}{\pi}\left(1-\frac{1}{\sqrt{M}}\right)\int_0^{\pi/2}\mathcal{M}_{\gamma_i}\left(\frac{g_{\text{QAM}}}{\sin^2\theta}\right)d\theta - \frac{4}{\pi}\left(1-\frac{1}{\sqrt{M}}\right)^2\int_0^{\pi/4}\mathcal{M}_{\gamma_i}\left(\frac{g_{\text{QAM}}}{\sin^2\theta}\right)d\theta, \quad (23)$$

where $g_{\text{QAM}} = 3/2(M-1)$.

3.3. General STANC Moment Generating Function. In this section, we derive the expressions for unconditional MGFs to evaluate the above-average SER for ANC communication over Nakagami-m, Rician, and Rayleigh fading channels. The MGF of γ_i is given as

$$\mathcal{M}_{\gamma_2}(s) = \mathbb{E}_{\alpha_{1j},\alpha_{2j}}\left(e^{-s\gamma_2}\right). \quad (24)$$

We assume that α_{1j} and α_{2j} are independent random variables. The MGF for given α_{2j} is represented as:

$$\mathcal{M}_{\gamma_2|\alpha_{2j}}(s) = \mathbb{E}_{\alpha_{1j}}\left(e^{-\sum_{j=1}^{L}(\beta_j^2\overline{\gamma}\alpha_{1j}\alpha_{2j}/(\beta_j^2\alpha_{2j}+1))s}\right). \quad (25)$$

3.3.1. For Nakagami-m Fading Channels. As $\alpha_{ij} = |h_{ij}|^2$ (for $i, j = \{1,2\}$) are gamma-distributed random variables, (25) can be written as

$$\mathcal{M}_{\gamma_2|\alpha_{2j}} = \prod_{j=1}^{L}\frac{1}{\left(1+\left(\beta_j^2\overline{\gamma}\alpha_{2j}/\left(\beta_j^2\alpha_{2j}+1\right)m\right)s\right)^m}. \quad (26)$$

Equation (25) can also be written as

$$\mathcal{M}_{\gamma_2|\alpha_{2j}} = \frac{1}{(1+(\overline{\gamma}/m)s)^{Lm}} \times \prod_{j=1}^{L}\left(\frac{\alpha_{2j}+\left(1/\beta_j^2\right)}{\alpha_{2j}+\left(1/\left(\beta_j^2+\left(\beta_j^2\overline{\gamma}/m\right)s\right)\right)}\right)^m. \quad (27)$$

Equation (27) can be further simplified as:

$$\mathcal{M}_{\gamma_2|\alpha_{2j}} = \frac{1}{(1+(\overline{\gamma}/m)s)^{Lm}}\prod_{j=1}^{L}\left(1+G\left(\alpha_{2j}\right)\right), \quad (28)$$

where $G(\alpha_{2j}) = g_{m-1}\alpha_{2j}^{m-1} + \cdots + g_1\alpha_{2j} + g_0/((\alpha_{2j}+(1/\beta_j^2+(\beta_j^2\overline{\gamma}/m)s))^m)$, with $g_{m-1},\ldots,g_1,g_0$ as real constants. The unconditional MGF is obtained by averaging (28) over α_{2j} and given as

$$\mathcal{M}_{\gamma_2}(s) = \frac{1}{(1+(\overline{\gamma}/m)s)^{Lm}} \times \prod_{j=1}^{L}\left(1+\sum_{v=1}^{m}m^m C_{v,j}\left(\frac{1}{\beta_j^2+\left(\beta_j^2\overline{\gamma}/m\right)s}\right)^{m-v} \times \psi\left(m, m-v+1, \frac{m}{\beta_j^2+\left(\beta_j^2\overline{\gamma}/m\right)s}\right)\right), \quad (29)$$

$$C_{v,j} = \frac{1}{(m-v)!}\frac{d^{m-v}}{d\alpha_{2j}^{m-v}} \times \left(\left(\alpha_{2j}+\frac{1}{\beta_j^2+\left(\beta_j^2\overline{\gamma}/m\right)s}\right)^m G\left(\alpha_{2j}\right)\right)\Bigg|_{\alpha_{2j}=-1/(\beta_j^2+(\beta_j^2\overline{\gamma}/m)s)}, \quad (30)$$

where, $C_{v,j}$ is given in (30), and $\psi(\cdot,\cdot,\cdot)$ is the confluent hypergeometric function of the second kind.

3.3.2. For Rician Fading Channels. The conditional MGF for given α_{2j} of the SNR for STANC over Rician fading channels is given by:

$$\mathcal{M}_{\gamma_2|\alpha_{2j}}(s) = \prod_{j=1}^{L}\frac{\left(1+K_{1j}\right)}{\left(1+K_{1j}\right)+\left(\beta_j^2\overline{\gamma}\alpha_{2j}/\left(\beta_j^2\alpha_{2j}+1\right)\right)s} \times \exp\left\{-\frac{K_{1j}\left(\beta_j^2\overline{\gamma}\alpha_{2j}/\left(\beta_j^2\alpha_{2j}+1\right)\right)s}{\left(1+K_{1j}\right)+\left(\beta_j^2\overline{\gamma}\alpha_{2j}/\left(\beta_j^2\alpha_{2j}+1\right)\right)s}\right\}, \quad (31)$$

where K_{1j} and K_{2j} are the Rician factor for link $T_1 \rightarrow R_j$ and $T_2 \rightarrow R_j$, respectively. The unconditional MGF is obtained by averaging (31) over $\alpha_{2\text{j}}$ and given as

$$\mathcal{M}_{\gamma_2}(s) = \prod_{j=1}^{L}\sum_{k=0}^{\infty}\sum_{n=0}^{k}\binom{k}{n}\frac{K_{2j}^{n}K_{1j}^{k-n}\left(1+K_{2j}\right)^{k-n}\left(1+K_{1j}\right)^{n-k}}{k!n!} \times \frac{\left(\beta_j^2\overline{\gamma}s\right)^{k-n}}{\left(\beta_j^2+\left(\beta^2\overline{\gamma}/\left(1+K_{1j}\right)\right)s\right)^{2k-2n+1}} \times \exp\left\{-K_{2j}-\frac{\left(K_{1j}/\left(1+K_{1j}\right)\right)\beta_j^2\overline{\gamma}s}{\beta_j^2+\left(\beta_j^2\overline{\gamma}/\left(1+K_{1j}\right)\right)s}\right\}$$

$$\times\left(\beta_j^2(n+1)\psi\left(k-n+1,\,k-2n;\frac{1+K_{2j}}{\beta_j^2+\left(\beta_j^2\overline{\gamma}/\left(1+K_{1j}\right)\right)s}\right)+\left(1+K_{2j}\right)\times\psi\left(k-n+1,\,k-2n+1;\frac{1+K_{2j}}{\beta_j^2+\left(\beta_j^2\overline{\gamma}/\left(1+K_{1j}\right)\right)s}\right)\right), \quad (32)$$

where $\psi(\cdot,\cdot,\cdot)$ is the confluent hypergeometric function of the second kind [20].

3.3.3. For Rayleigh Fading Channels. The unconditional MGF of the SNR for $K = 0$ or $m = 1$ (special case: Rayleigh) is given as

$$\mathcal{M}_{\gamma_2}(s)=\prod_{j=1}^{L}\beta_j^2 k_j\left(e^{k_j}Ei\left(-k_j\right)\left(k_j-\frac{1}{\beta_j^2}\right)+1\right), \quad (33)$$

where $k_j = (1/\beta_j^2(1+\overline{\gamma}s))$ and $Ei(\cdot)$ is an exponential integral function.

4. Ergodic Capacity Analysis

The ergodic capacity is the expectation of the information rate over the channel distribution between the source and destination and is defined in [21] as

$$C_{\text{erg}}=\mathbb{E}\left\{\frac{1}{L}\log(1+\gamma_2)\right\}, \quad (34)$$

which is upper bounded by Jensen's Inequality in [22] and is given as:

$$C_{\text{erg}}\leq\frac{1}{L}\log(1+\mathbb{E}\{\gamma_2\}). \quad (35)$$

It is more important to determine the capacity of STANC two-way channels in a multipath fading environment. In this context, we propose that the STANC channel ergodic capacity can be accurately approximated by a Gaussian random variable, for the case where the channel state information (CSI) is not available at the transmitter but the receiver has the perfect channel state information. We present the ergodic capacity analysis of STANC two-way relay network based on the Gaussian approximation [13] under Nakagami and Rician fading channels. The implication of this Gaussian approximation is that only the capacity mean and variance are required to obtain an accurate approximation even for a lower number of relays, for various fading scenarios, and with a wide range of transmitting signal-to-noise ratio (TSNR). We resort to the numerical computation approach by using the Taylor expansion of $\ln[1+\mathbb{E}\{\gamma_{ij}\}]$ with the mean of $\mathbb{E}\{\gamma_{ij}\}$ to obtain the second-order approximation expression for C_{erg} given in [23] as:

$$C_{\text{erg}}\approx\frac{1}{L}\log_2 e\left(\ln\left[1+\sum_{j=1}^{L}\mathbb{E}\left\{\gamma_{ij}\right\}\right]-\frac{\sum_{j=1}^{L}\mathbb{E}\left\{\gamma_{ij}^2\right\}}{2\left(1+\sum_{j=1}^{L}\mathbb{E}\left\{\gamma_{ij}\right\}\right)^2}+\frac{2\sum_{j=1}^{L}\sum_{k=j+1}^{L}\mathbb{E}\left\{\gamma_{ij}\right\}\mathbb{E}\{\gamma_{ik}\}}{2\left(1+\sum_{j=1}^{L}\mathbb{E}\left\{\gamma_{ij}\right\}\right)^2}-\frac{\left(\sum_{j=1}^{L}\mathbb{E}\left\{\gamma_{ij}\right\}\right)^2}{2\left(1+\sum_{j=1}^{L}\mathbb{E}\left\{\gamma_{ij}\right\}\right)^2}\right), \quad (36)$$

where γ_2 is given by (21) and $\gamma_{ij} = (\overline{\gamma}\beta_j^2|h_{1j}|^2|h_{2j}|^2/(\beta_j^2 h_{ij}|^2+1))$, and γ_{ij} is the equivalent SNR at terminal T_i from jth relay in second phase of STANC bidirectional scheme. Now, the mean and second moment of γ_{ij} can be given as:

$$\mathbb{E}\left\{\gamma_{ij}\right\}=\int_0^\infty\gamma_{ij}f\left(\alpha_{ij}\right)d\gamma_{ij},\qquad \mathbb{E}\left\{\gamma_{ij}^2\right\}=\int_0^\infty{\gamma_{ij}}^2 f\left(\alpha_{ij}\right)d\gamma_{ij}. \quad (37)$$

The probability density function of α_{ij} in case of Nakagami-m distribution is given in [17] as:

$$f\left(\alpha_{ij}\right)=\frac{m^m\alpha_{ij}^{m-1}}{\Gamma(m)}\exp\left(-m\alpha_{ij}\right), \quad (38)$$

where $\alpha_{ij} = |h_{ij}|^2$, $\Gamma(\cdot)$ is a gamma function. Here we consider $\mathbb{E}(|h_{ij}|^2) = 1$, where $\mathbb{E}(\cdot)$ is the expectation operator. For $m = 1$, the Nakagami-m distribution becomes the exponential distribution.

Using [18, equation (2.15)], the probability density function of α_{ij} for Rician distribution is given as:

$$f\left(\alpha_{ij}\right)=\left(1+K_{ij}\right)\exp\left(-\left(1+K_{ij}\right)\alpha_{ij}-K_{ij}\right)\times I_0\left(2\sqrt{\left(K_{ij}\left(1+K_{ij}\right)\right)\alpha_{ij}}\right), \quad (39)$$

where $I_0(\cdot)$ is the zero-th order modified Bessel function of the first kind and K_{ij} is the Rician fading factor for the link from ith to jth terminal. For $K_{ij} = 0$, the Ricean distribution becomes the Rayleigh distribution. Now, by substituting (38) in (37), the mean and second moment of γ_{ij} over Nakagami-m fading channels are respectively given by

$$\mathbb{E}\left\{\gamma_{ij}\right\}=\frac{m^{m+1}}{\beta_j^{2m}}\overline{\gamma}\exp\left\{\frac{m}{\beta_j^2}\right\}\Gamma\left(-m,\frac{m}{\beta_j^2}\right), \quad (40)$$

$$\mathbb{E}\left\{\gamma_{ij}^2\right\}=\frac{\overline{\gamma}^2 m^m(1+m)^2}{\beta_j^{2m}}\psi\left(m+2,\,m+1;\frac{m}{\beta_j^2}\right), \quad (41)$$

where $\psi(\cdot,\cdot,\cdot)$ denotes the confluent hypergeometric function of the second kind. Similarly, by substituting (39) in (37) we compute the mean and second moment of γ_{ij} over Rician-K fading channels as given in (42) and (43), respectively.

$$\mathbb{E}\left\{\gamma_{ij}\right\} = \sum_{n=0}^{\infty}\frac{\overline{\gamma}}{\beta_j^{2n+2}}\frac{K_{ij}^n\left(1+K_{ij}\right)^{n+1}}{(n!)^2}\exp\left\{-K_{ij}+\frac{1+K_{ij}}{\beta_j^2}\right\} \times\Gamma(n+2)\Gamma\left(-1-n,\frac{1+K_{ij}}{\beta_j^2}\right), \tag{42}$$

$$\mathbb{E}\left\{\gamma_{2j}^2\right\} = \sum_{n=0}^{\infty}\frac{\overline{\gamma}^2}{\beta_j^{2n+2}}\frac{K_{2j}^n\left(1+K_{2j}\right)^{n+1}\left(2+4K_{1j}+K_{1j}^2\right)\left(1+K_{1j}\right)^{-2}}{(n!)^2} \times\Gamma(n+3)\psi\left(n+3,n+2;\frac{1+K_{2j}}{\beta_j^2}\right). \tag{43}$$

Consequently, the second-order approximated ergodic capacity for amplify and forward (AF) of STANC two-way relay network systems can be obtained by substituting (40), (41) and (42), (43) in (36) for Nakagami and Rician fading channels, respectively.

5. Results and Discussions

Numerical study results illustrate the performance and capacity analysis of our proposed STANC system. The exact SER and ergodic capacity performance are analytically derived in Section 3 and 4, respectively, and are drawn by using Mathematica software and shown together with the results obtained from Monte Carlo simulations. We obtained the analytical results for SER performance by substituting (29) and (32) in (22) and (23) for Nakagami and Rician fading channels, respectively. Similarly, we obtain analytical results for ergodic capacity as discussed in Section 4 for Nakagami and Rician fading channels. All the SER and capacity results are drawn w.r.t. the average SNR.

We initially present the SER performance of the two sources in the two-way relay network. Since, the SER performance at T_1 and T_2 are symmetrical, therefore, for simplicity, we compute the SER performance only at T_2. We assume that the channel coefficients remain constant during the time slots for transmission from terminals to relay and relay to terminals. Perfect channel estimation is assumed at the receiver, but transmitter does not know the channel conditions in terms of CSI. The uncorrelated propagation channel coefficients are Rayleigh, Nakagami, and Rician distributed. We consider the three types of ideal coherent modulation/demodulation schemes that is: BPSK, QPSK, and 16-QAM. The analysis is performed in terms of symbol error rate (SER). As a future work, this work can be extended to analyze the performance of the proposed STANC networks by taking path loss and shadowing effect into consideration.

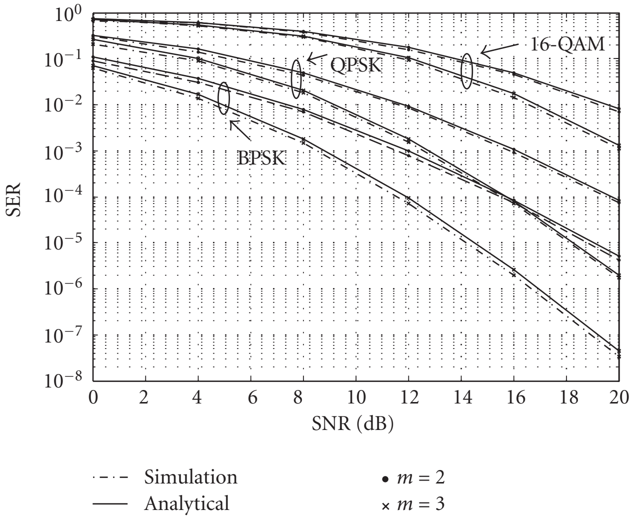

Figure 2: SER analysis of STANC over Nakagami-m fading channels with different constellation size and orthogonal transmission from the relays ($L = 2$).

5.1. SER Performance. Figures 2 and 3 show a good agreement between numerical analysis and simulation results for Nakagami $m = 2,3$ and Rician $K = 1,5,10$ fading channels, respectively. A negligible difference can be seen in numerical and Monte-Carlo simulation results because at relatively high SNR values it was not possible to compute the numerical integration, since the crossing points no longer exist. At such points, numerical integration errors start to appear. These curves present the performance of the system with 2 relays operating in AF mode. In this case, at the destination end, each received signal carry data-modulated symbol which is exploited through STANC to obtain spatial-diversity gain resulting in improved performance. The figures also illustrate that the performance of STANC improves due to the channel coding gain in a block frequency flat-fading channel. It can be seen from Figures 2, 3, and 4 that the average SER exhibits decreasing coding gain as the constellation size increases for example, BPSK, QPSK, and 16-QAM, while full diversity is always achieved for sufficiently higher SNR. The coding gain can be certainly improved by invoking error control coding (ECC) at the expense of rate loss.

Figure 4 shows the performance improvement achieved in case of STANC-based transmission compared to ANC for SER $= 10^{-2}$, the SNR (E_b/N_0) gain of approximately 10 dB is achieved in Rayleigh fading channels. It can be seen from the figure that the E_b/N_0 gain of STANC is more for lower SER when compared to ANC scheme without STC and the dependence of the SER performance on the E_b/N_0 with the number of channel links L (L = no. of relays). The performance of STANC increases as L increases owing to more spatial diversity gain. The figure also shows the SER curves for STANC and OSTANC by implementing Alamouti codes 2×2 and OSTBC codes 3×4 for $L = 2$ and $L = 3$, respectively, for BPSK, QPSK, and 16QAM.

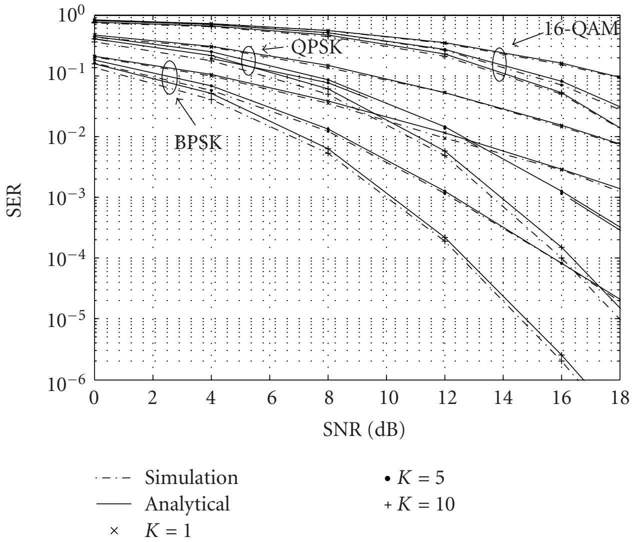

Figure 3: SER analysis of STANC over Rician fading channels with different constellation size and orthogonal transmission from the relays ($L = 2$).

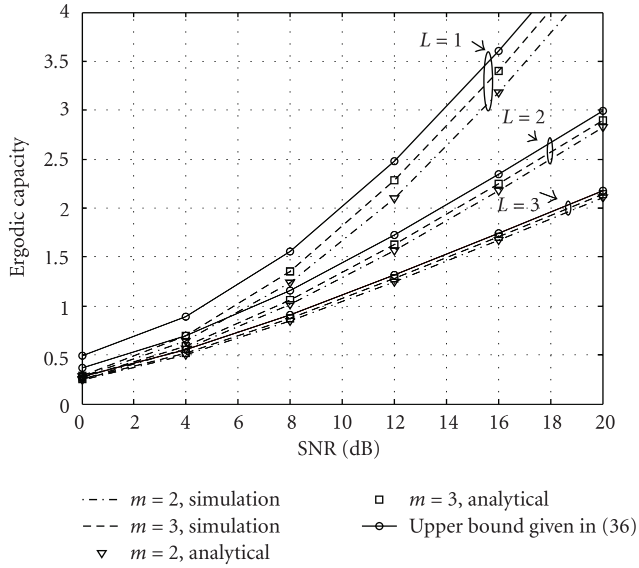

Figure 5: Ergodic capacity analysis of STANC over Nakagami-m fading channels. The approximated analytical results given in (36) using (40) and (41).

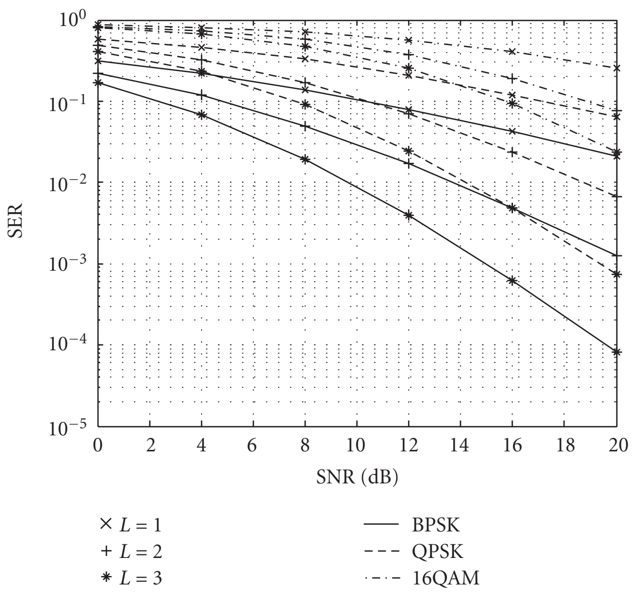

Figure 4: Performance comparison of STANC and ANC schemes over Rayleigh fading channels.

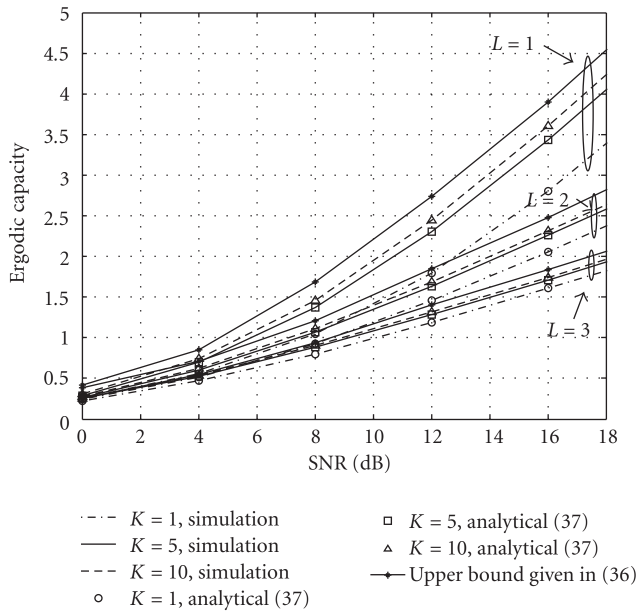

Figure 6: Ergodic capacity analysis of STANC over Rician fading channels with upper bound tightness given in (35) using (42) with increasing number of relays.

5.2. Ergodic Capacity. Analytically, the upper bound is derived from Jensen's inequality approach for Nakagami and Rician fading as in [22], which discussed only the Rayleigh fading channel. The ergodic capacity can be upper bounded by (35) because of concavity and with (40) and (42), this upper bound can be evaluated for Nakagami and Rician fading channels, respectively. The capacity given in (36) is evaluated using Monte Carlo numerical computational method to investigate the accuracy of the Gaussian approximations in a Nakagami and Rician fading environment. It can be seen from Figures 5 and 6 that the approximate ergodic capacity expressions of (36) are very stringent. The difference is negligible with the increase in the number of relays and in practical SNR regions. With a fewer number of relays, the simple upper bound is not so tight.

Figures 5 and 6 also illustrate the achievable ergodic capacity over Nakagami $m = 2, 3$ and Rician $k = 1, 5, 10$, respectively, as a function of the Eb/N_0 with number of paths (Relays) $L = 1, 2, 3$ for (i) analog network coding (ANC), (i.e., single source, destination terminal with single relay), (ii) analog network coding with space-time Alamouti codes 2 × 2 (STANC), and (iii) analog network coding with orthogonal space time OSTBC codes 4 × 3 (OSTANC). It can be observed that STANC is defined as 2 terminals communicating with each other through 2 relays by using Alamouti codes and 3, 4 relays by using OSTBC codes in the case of OSTANC. Both the source and destination terminals fully exploit the two-way transmission scheme of ANC and transmit their signals simultaneously to the relays in the first stage and receive the interfered signal from the relays in the second stage. Figures 5 and 6 show that the ergodic capacity of analog network coding (ANC), that is, single source, destination terminal with single relay is considerably increased in comparison with STANC and OSTANC scheme. This is because of the orthogonal partitioning of system resources. In ANC, the total available transmit power is divided only among the source terminals and the single relay whereas in STANC relaying, the total power is divided among the source terminals and also increasing number of relay terminals that is, $L = 2, 3$. It can also be observed from the figures that the performance of the networks involving more number of relays that is, STANC and OSTANC is considerably better than ANC due to the gain obtained through diversity combining.

6. Conclusion

In this paper, the novel extension of analog network coding based on space-time coding technique in multiple relay network under different fading scenarios is presented. The SER of M-ary QAM and PSK modulated signals are evaluated using the derived MGF expressions over Nakagami-m and Rician fading channels. The approximate closed-form expressions of ergodic capacity are derived for STANC system. Numerical results indicate that all the approximate analytical expressions derived are very tight and can be effectively used for performance and capacity analysis of the proposed STANC system by arbitrarily changing different parameters of interest and in any SNR region. The analysis shows that the STANC system has significant performance improvement compared to ANC due to the diversity of combining. Reduction in ergodic capacity performance is also observed due to the orthogonal partitioning of system resources.

References

[1] P. E. Mogensen, T. Koivisto, K. I. Pedersen et al., "LTE-advanced: the path towards gigabit/s in wireless mobile communications," in *Proceedings of the 1st International Conference on Wireless Communication, Vehicular Technology, Information Theory and Aerospace and Electronic Systems Technology, Wireless (VITAE '09)*, pp. 147–151, Aalborg, Denmark, May 2009.

[2] V. Genc, S. Murphy, Y. Yu, and J. Murphy, "IEEE 802.16j relay-based wireless access networks: an overview," *IEEE Wireless Communications*, vol. 15, no. 5, pp. 56–63, 2008.

[3] S. A. K. Tanoli, I. Khan, and N. Rajatheva, "Cooperative Networks: bitinterleavedcoded modulation with iterative decoding," *Journal of Communications*, vol. 5, no. 7, pp. 562–570, 2010.

[4] S. A. K. Tanoli, I. Khan, and N. Rajatheva, "Performance comparison of BICM-ID and BILDPCM-ID based cooperative network," in *Proceedings of the 72nd IEEE Vehicular Technology Conference (VTC '10)*, Ottawa, Canada, September 2010.

[5] R. Ahlswede, N. Cai, S.-Y. R. Li, and R. W. Yeung, "Network information flow," *IEEE Transactions on Information Theory*, vol. 46, no. 4, pp. 1204–1216, 2000.

[6] P. Popovski and H. Yomo, "Bi-directional amplification of throughput in a wireless multi-hop network," in *Proceedings of the 63rd Vehicular Technology Conference (VTC '06)*, vol. 2, pp. 588–593, Melbourne, Australia, May 2006.

[7] S. Zhang, S. C. Liew, and P. P. Lam, "Hot topic: physical-layer network coding," in *Proceedings of the 12th Annual International Conference on Mobile Computing and Networking (MOBICOM '06)*, pp. 358–365, Los Angeles, Calif, USA, September 2006.

[8] S. Zhang, S. C. Liew, and L. Lu, "Physical layer network coding schemes over finite and infinite fields," in *Proceedings of IEEE Global Telecommunications Conference (GLOBECOM '08)*, pp. 3784–3789, New Orleans, La, USA, November-December 2008.

[9] T. Wang and G. B. Giannakis, "Complex field network coding for multiuser cooperative communications," *IEEE Journal on Selected Areas in Communications*, vol. 26, no. 3, pp. 561–571, 2008.

[10] S. Katti, S. Gollakota, and D. Katabi, "Embracing wireless interference: analog network coding," in *Proceeding of ACM Conference on Computer Communications (SIGCOMM '07)*, pp. 397–408, Kyoto, Japan, August 2007.

[11] S. Katti, I. Marić, A. Goldsmith, D. Katabi, and M. Medard, "Joint relaying and network coding in wireless networks," in *Proceedings of IEEE International Symposium on Information Theory (ISIT '07)*, pp. 1101–1105, Nice, France, June 2007.

[12] B. Rankov and A. Wittneben, "Spectral efficient protocols for half-duplex fading relay channels," *IEEE Journal on Selected Areas in Communications*, vol. 25, no. 2, pp. 379–389, 2007.

[13] H. Gacanin and F. Adachi, "Broadband analog network coding," *IEEE Transactions on Wireless Communications*, vol. 9, no. 5, Article ID 5463213, pp. 1577–1583, 2010.

[14] L. Song, Y. Li, A. Huang, B. Jiao, and A. V. Vasilakos, "Differential modulation for bidirectional relaying with analog network coding," *IEEE Transactions on Signal Processing*, vol. 58, no. 7, pp. 3933–3938, 2010.

[15] T. Cui, F. Gao, T. Ho, and A. Nallanathan, "Distributed space-time coding for two-way wireless relay networks," *IEEE Transactions on Signal Processing*, vol. 57, no. 2, pp. 658–671, 2009.

[16] F. Gao, T. Cui, and A. Nallanathan, "On channel estimation and optimal training design for amplify and forward relay networks," *IEEE Transactions on Wireless Communications*, vol. 7, no. 5, Article ID 4524288, pp. 1907–1916, 2008.

[17] S. Atapattu, N. Rajatheva, and C. Tellambura, "Performance analysis of TDMA relay protocols over Nakagami-m fading," *IEEE Transactions on Vehicular Technology*, vol. 59, no. 1, pp. 93–104, 2010.

[18] M. K. Simon and M.-S. Alouini, *Digital Communication over Fading Channels*, John Wiley & Sons, New York, NY, USA, 2005.

[19] V. Tarokh, N. Seshadri, and A. R. Calderbank, "Space-time codes for high data rate wireless communication: performance criterion and code construction," *IEEE Transactions on Information Theory*, vol. 44, no. 2, pp. 744–765, 1998.

[20] I. S. Gradshteyn and I. M. Ryzhik, *Table of Integrals, Series and Products*, Academic Press, New York, NY, USA, 6th edition, 2000.

[21] J. G. Proakis, *Digital Communications*, McGraw-Hill, New York, NY, USA, 3rd edition, 1995.

[22] G. Farhadi and N. C. Beaulieu, “Ergodic capacity of multi-hop wireless relaying systems in rayleigh fading,” in *Proceedings of IEEE Global Telecommunications Conference (GLOBECOM ’08)*, pp. 4477–4482, usa, November-December 2008.

[23] S. Chen, W. Wang, and X. Zhang, “Ergodic and outage capacity analysis of cooperative diversity systems under rayleigh fading channels,” in *Proceedings of IEEE International Conference on Communications Workshops (ICC ’09)*, June 2009.